Hindawi Publishing Corporation
International Journal of Photoenergy
Volume 2016, Article ID 9270492, 9 pages
http://dx.doi.org/10.1155/2016/9270492

Research Article

Flexible Bench-Scale Recirculating Flow CPC Photoreactor for Solar Photocatalytic Degradation of Methylene Blue Using Removable TiO_2 Immobilized on PET Sheets

Doaa M. EL-Mekkawi,[1] Norhan Nady,[2] Nourelhoda A. Abdelwahab,[3] Walied A. A. Mohamed,[4] and M. S. A. Abdel-Mottaleb[5]

[1]*Physical Chemistry Department, National Research Centre (NRC), 33 Elbohouth Street, P.O. Box 12622, Dokki, Giza, Egypt*
[2]*Polymeric Materials Research Department, Advanced Technology and New Materials Research Institute (ATNMRI), City of Scientific Research and Technological Applications (SRTA-City), New Borg El-Arab City, Alexandria 21934, Egypt*
[3]*Polymers and Pigments Department, National Research Centre (NRC), 33 Elbohouth Street, P.O. Box 12622, Dokki, Giza, Egypt*
[4]*Inorganic Chemistry Department, National Research Centre, 33 Elbohouth Street, P.O. Box 12622, Dokki, Giza, Egypt*
[5]*Nano-Photochemistry and Solar Chemistry Department, Laboratory of Chemistry, Faculty of Science, Ain Shams University, Abbassia, 11566 Cairo, Egypt*

Correspondence should be addressed to Doaa M. EL-Mekkawi; doaa_egypt@yahoo.com

Received 30 December 2015; Revised 8 February 2016; Accepted 10 February 2016

Academic Editor: Giovanni Palmisano

TiO_2 immobilized on polyethylene (PET) nonwoven sheet was used in the solar photocatalytic degradation of methylene blue (MB). TiO_2 Evonik Aeroxide P25 was used in this study. The amount of loaded TiO_2 on PET was approximately 24%. Immobilization of TiO_2 on PET was conducted by dip coating process followed by exposing to mild heat and pressure. TiO_2/PET sheets were wrapped on removable Teflon rods inside home-made bench-scale recirculating flow Compound Parabolic Concentrator (CPC) photoreactor prototype (platform $0.7 \times 0.2 \times 0.4\,m^3$). CPC photoreactor is made up of seven low iron borosilicate glass tubes connected in series. CPC reflectors are made of stainless steel 304. The prototype was mounted on a platform tilted at 30°N local latitude in Cairo. A centrifugal pump was used to circulate water containing methylene blue (MB) dye inside the glass tubes. Efficient photocatalytic degradation of MB using TiO_2/PET was achieved upon the exposure to direct sunlight. Chemical oxygen demand (COD) analyses reveal the complete mineralization of MB. Durability of TiO_2/PET composite was also tested under sunlight irradiation. Results indicate only 6% reduction in the amount of TiO_2 after seven cycles. No significant change was observed for the physicochemical characteristics of TiO_2/PET after the successive irradiation processes.

1. Introduction

Semiconductor photocatalysis is a fast growing area in terms of both research and commercial activities [1]. In recent years, supported TiO_2 materials have been widely studied for the application on both indoor and outdoor air and water purification [2–5] disinfection and antibacteria [6, 7], as well as self-cleaning surface [8, 9].

Generally, photocatalytic oxidation follows the absorption of energy photons by semiconductors such as TiO_2. Each photon should have energy ($h\nu$) more than or equal to the bandgap energy of TiO_2. The absorbed photon then promotes the excitation of electron (e^-) from valence band to conduction band. The generated electrons on conduction band and holes on valence band (h^+) would then directly or indirectly interact with adsorbed organic pollutants causing their destruction. UVA light energy (wavelength between 300 and 400 nm) is adequate to perform the photocatalytic oxidations on TiO_2 surfaces. Solar energy is a free sustainable source UVA light energy. Egypt has UVA irradiances that reach $40\,W/m^2$ or even higher on sunny days [10].

Compound Parabolic Concentrator (CPC) has been extensively interpreted as a good option for solar photochemical applications [11–16]. CPC reactor consists of cylindrical

absorber, on a combined reflecting profile. The reflector geometry mixes two parabolas and one involute whose curves relate to the diameter of the circle and to the concentration ratio.

Titanium dioxide can be used as slurry or fixed inside the CPC photocatalytic reactors. The major obstacle for the practical use of TiO_2 slurries in water treatment was the requirement for the expensive liquid-solid separation. This would consume more efforts, money, and time. In addition, the recovery loss of catalyst might be high [17]. Therefore, catalyst immobilization is the key for successful implementation of heterogeneous photocatalytic oxidation of organic pollutants in water [18, 19].

Some commonly used substrates such as glass, aluminum, and stainless steel are suitable for high temperature annealing treatment after the photocatalyst loading. However, the stiffness and weight of the materials impose limitations for large-scale implementation.

Different methods have been developed on loading of TiO_2 on polymeric sheets from photocatalyst suspensions [20]. All these approaches have to fulfill at least three main needs: the long term stability of the photocatalyst immobilization, its availability for heterogeneous photocatalysis, and the low cost of the deposition procedure, in view of a practical application.

Loading methods, such as sputtering [21, 22], electrochemical deposition [23], spin coating [24], and electrophoretic coating [25], have been previously utilized for the preparation of titania supported thin films. However, these methods are often complicated, costly, and difficult for practical application [26, 27]. Large-scale application of photocatalytic oxidation for water purification can be achieved through direct coating of commercial photocatalysts such as Degussa P25 TiO_2 [28]. When using direct coating, the primary issue of interest is the stability of the coating. Poor adhesions have been reported by direct coating method such as dip coating or spin coating [29, 30], where even slight mechanical abrasion may remove the photocatalyst from the substrate surface. Thus, a binding agent is usually necessary for direct coating in order to form solid adhesion between catalyst and substrate. Either organic polymer or inorganic binding materials have been used for photocatalyst immobilization [31–33]. However, the binder amount may affect the photocatalytic oxidation activity and stability of the coating [34].

Evaluation of the photocatalytic activity of surfaces modified photocatalysts is a crucial point. The dye method is one of the most commonly used methods for the evaluation of the photocatalytically active surfaces. Methylene blue (MB) has been widely addressed as a test pollutant in the evaluation of the photocatalytic activity of semiconductors. MB is extensively used as textile and leather and paper dye. It has been previously demonstrated that films of titania were able to mediate the complete photomineralization of MB [35]. With MB as a highly colored organic material, all what is required for the evaluation process is following up its rate of photocatalytic bleaching via UV/vis spectrophotometery [36, 37]. Recently, the international standards organization (ISO) released a technical standard (ISO 10678:2010) for "determination of photocatalytic activity of surfaces in an aqueous medium by degradation of methylene blue" [1].

In this work, a bench-scale solar CPC photoreactor has been designed and fabricated for testing the photocatalytic oxidation of organic pollutants. TiO_2 Evonik Aeroxide P25 (previously known as Degussa P25) supported on PET sheets was used as a photocatalytically active surface inside the reactor. Immobilization of TiO_2 on PET was conducted by a simple and cost effective method. MB aqueous solutions were used to study the photocatalytic activity of TiO_2/PET sheets under sunlight. COD analyses were conducted to test the complete mineralization of MB. Durability of TiO_2/PET composite was also tested under sunlight irradiation. The physicochemical characterizations of the prepared TiO_2/PET composite before and after degradation processes were also investigated.

2. Materials and Methods

2.1. Chemicals. TiO_2 Evonik Aeroxide P25 (surface area 50 m^2/g) is used as photocatalyst and was provided by Evonik Industries AG, Germany. Polyethylene terephthalate substrates used in this work are nonwoven fabrics, with overall packing density of 0.055 g/cm^3. Methylene blue (MB), $C_{16}H_{18}ClN_3S{\cdot}xH_2O$, 96%, provided by Fluka, was used as received.

2.2. Preparation of PET/TiO_2 Composite. PET/TiO_2 composite was prepared by dip coating of PET textile substrate with TiO_2. In this study, strips of dimensions (0.2 × 0.7 m^2) were cut, weighed, and then immersed in double distilled water for 20 min. Concentrated TiO_2 Aeroxide P25 solution in double distilled water was prepared. The preweighed samples were immersed separately in this solution for 1 h. The wet TiO_2-loaded PET substrates were pressed at 60°C for 20 min. The percentage of loaded TiO_2 was determined and the samples were washed with distilled water several times, and after each time the TiO_2 content was calculated as follows:

$$TiO_2 \text{ content\%} = \frac{W_2 - W_1}{W_1} \times 100, \quad (1)$$

where W_1 and W_2 are the weights of PET substrate before and after TiO_2 loading.

2.3. Characterizations of PET/TiO_2 Composite

2.3.1. Fourier Transform Infrared (FT-IR) Spectra. The characteristic functional groups of TiO_2 and PET and PET/TiO_2 composite and UV-irradiated PET/TiO_2 composite were investigated by Jasco 3400 FT-IR spectrophotometer, in the range of 4000–400 cm^{-1}.

2.3.2. Scanning Electron Microscope (SEM). In SEM measurements, an electron beam was passed through the specimens followed by scattering them back as electrons and secondary electrons. Backscattered secondary electrons were used to form the image on the computer monitor. The acceleration of the electron beam was 10 kV. This was carried out on Quanta FEG250 Instrument.

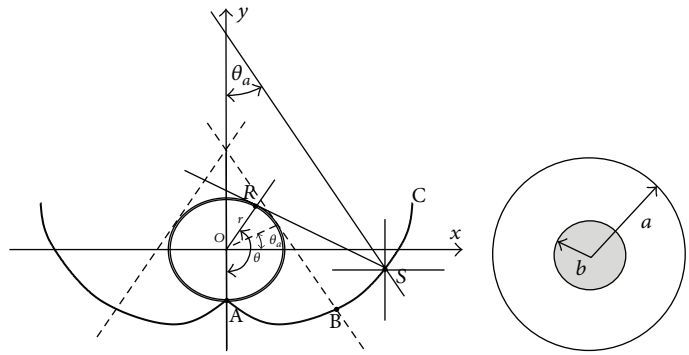

(a) (b)

Figure 1: (a) CPC acceptance angles, (b) Schematic cross section representation of used annulus to flow the wastewater [38].

2.3.3. Energy Dispersive X-Ray (EDX). The spectra of TiO_2 coated PET fabrics before and after UV irradiation were obtained by EDX measurements. A field emission scanning electron microscope (QUANTA FEG 250) coupled with an energy dispersive X-ray spectrometer (EDX) unit was employed to evaluate the elemental composition of TiO_2/PET sheets. Semiquantitative analyses in the inspection field were conducted using ZFA software where the energy of the emitted electrons for each element was counted in units of weight percent.

2.4. CPC Design

2.4.1. Pipeline Calculations. Compound Parabolic Concentrator (CPC) prototype is made up of seven tubes connected in series, and water would flow from the lowest (the nearest to the ground) to the highest tube and then to a tank. It has been mounted on a platform tilted (30°N local latitude in Cairo). A centrifuge pump was used to circulate wastewater. Rods of temperature-resistant Teflon were used as support for titanium dioxide immobilized in polymer films. These rods were fitted in the middle of glass tubes used to flow the wastewater. As shown in Figure 1(b), the cross-sectional area of annulus A was calculated using $\pi(a^2 - b^2)$, while the wetted perimeter was $2\pi(a + b)$. So, the equivalent diameter is $D_e = 4(\pi(a^2 - b^2)/2\pi(a + b)) = 2(a - b)$. The values of $2a$ (the inner diameter of glass tube) and $2b$ (the diameter of support Teflon rod) are specified depending on the required productivity and the limits of light penetration. The Reynolds number can be calculated using equivalent diameter D_e from $R_e = D_eV\rho/\mu$ in which ρ is the density and μ is the dynamic viscosity of used wastewater [39, 40]. The flow is specified in laminar region, and the friction factor f (for plastic surface) can be calculated from $= C/R_e$, where C is a constant, which depends on the ratio a/b [41]. The glass surface is smooth. The head loss is obtained by using $h_f = 2f(L/D_e)(V^2/g)$ and $\Delta P = 2f(L/D_e)(\rho V^2)$. Power to fluid is calculated from $\dot{m}h_f g$ in which mass flow rate $\dot{m}$ can be obtained from $\dot{m} = \rho VA$. Minor losses of connectors (T and U elbows) between tubes and inlet and outlet were included. The expansion and contraction effects were kept at minimum. The efficiency of the used pump was assumed to be 0.85.

Each tube with 0.25 m length (0.18 m exposed to the sunlight) was made from low iron borosilicate glass [$((3 \times 10^{-6})/K)$ coefficient of thermal expansion and 1.51–1.54 refractive index]. Seven tubes were connected in series with total irradiated surface 1.26 m^2 and volume equal to 0.723×10^{-3} m^3. The inner diameter of each borosilicate tube is 0.025 m (with 0.015 m glass thickness) and the diameter of the Teflon rod is 0.01 m. The Reynolds number is specified as 700 with average velocity 0.031 m/s. Total volume of the system is 2.5×10^{-3} m^3. The used volumetric flow rate using a centrifugal pump was 0.072 m^3/s and the irradiation time per cycle was about 4900 s.

2.4.2. Reflector Design. The reflectors of CPC were designed using the general equation of acceptance angles [38]:

$$\delta = r\theta \quad \text{For } |\theta| \le \theta_a + \frac{\pi}{2} \text{ Part AB in Figure 1(a)} \tag{2a}$$

$$\delta = r\frac{\theta + \theta_a + \pi/2 - \cos(\theta - \theta_a)}{1 + \sin(\theta - \theta_a)} \tag{2b}$$

$$\text{For } \theta_a + \frac{\pi}{2} \le |\theta| \le \frac{3\pi}{2} - \theta_a \text{ Part BC in Figure 1(a).}$$

δ is the distance of $\overline{RS}$, θ_a is the half angle of acceptance, and the CPC concentration ratio is given by:

$$C_{\text{cpc}} = \frac{1}{\sin\theta_a}. \tag{3}$$

The reflectors are made of stainless steel 304 with 8×10^{-4} m thickness. Concentration ratio that equals one and 90 degrees' acceptance half angle (θ_a) were used. Dimension of the collector is 0.17 m width and 0.2 m length.

2.4.3. The Fabricated Bench-Scale Recirculating Flow CPC. The photoreactor has been designed in small bench-scale dimensions (platform = $0.7 \times 0.2 \times 0.4$ m^3), so it facilitates conducting lab-scale experiments (see Figure 2). Almost all the parts are flexible. The Teflon rods are removable so several kinds of supported photocatalysts can be used. Moreover, experiments containing slurry photocatalysts can also be conducted. T connectors were used to obtain a flexible lab-scale system (use only one tube or more and withdrawing sample at any tube is possible).

(a) (b)

Figure 2: Fabricated bench-scale CPC photoreactor was used in this work. It contains seven low iron borosilicate tubes connected in series (a). Each tube was fixed on a reflector fabricated from stainless steel grade 304 (b). T connectors were used to obtain a flexible lab-scale system (use only one tube or more and withdrawing sample at any tube is possible). The simulated wastewater is fed from the lower tube to the upper one against the gravity using centrifuge pump connected to 4-L stirrer tank (not shown). The output treated wastewater was circulated to the tank (closed system). TiO_2 immobilized on PET sheets were wrapped on temperature-resistant removable Teflon rods hanged in the middle of each glass tube.

2.5. Measurement of Solar UV Irradiance. The UV light intensity was measured by YK-35UV radiometer, Taiwan. The radiometer had the same inclination as that of the platform where experiments were conducted.

2.6. Photocatalytic Degradation Experiments. All the experiments were carried out under direct sun irradiation at the roof of the National Research Centre, Cairo, Egypt (latitude 30°N, longitude 31°E) [10]. The initial concentration of MB solution was 1.5×10^{-5} M. The total volume (V_T) of the treated MB solution was 2.5 L. This volume is divided into two parts: the total irradiated volume (in glass tubes) (V_i) is 0.723 L and the dead reactor volume (i.e., connectors, tank, pipes, etc.). Prior to the degradation experiments, the photoreactor was covered with black plastic to permit the dark adsorption equilibrium of MB onto TiO_2/PET. After 30 min the plastic cover is removed and the reactor was exposed to the sunlight. The total exposure time for each experiment was approximately 7 hours, with exposure started at 9:00 and finishing at 16:00. During experiments, the MB solution was pumped at flow rate of 1.2 L/min through the glass tubes and finally into the recirculating tank. 4 mL of MB solution was collected for analysis from the reactor tank at timed intervals (1 h) during the degradation experiment.

Durability of the TiO_2/PET sheets was also tested for seven days. The photocatalytic degradation experiment was repeated as mentioned previously using the same TiO_2/PET sheets. Fresh solutions of MB were used at each repetition. The collected data at each day were interpreted using the following equation [42]:

$$t_{30\,\mathrm{w},n} = t_{30\,\mathrm{w},n-1} + \Delta t_n \left(\frac{\overline{\mathrm{UV}}}{30}\right)\left(\frac{V_i}{V_t}\right), \qquad \Delta t_n = t_n - t_{n-1}, \tag{4}$$

where t_n is the experimental time for each sample, $\overline{\mathrm{UV}}$ is the average solar ultraviolet radiation measured during Δt_n, and $t_{30\,\mathrm{w}}$ is a normalized illumination time. In this case, time refers to a constant solar UV power of 30 W/m^2 (typical solar UV power on a perfectly sunny day around noon).

The initial amounts of adsorbed MB molecules on TiO_2/PET sheets at each repetition were calculated as follows:

$$\text{Amount of adsorbed MB} = \frac{C_{0\mathrm{B}} - C_{0\mathrm{A}}}{\mathrm{SN}}, \tag{5}$$

where $C_{0\mathrm{B}}$ and $C_{0\mathrm{A}}$ are the concentrations of MB in solution before and after the dark adsorption, respectively. The values of $C_{0\mathrm{B}}$ and $C_{0\mathrm{A}}$ of MB solutions are spectrophotometrically measured at $\lambda_{\max} = 665$ nm. S is the area of PET strip and N is the number of strips (seven strips).

2.7. UV/Visible Measurements. The change in MB color during the degradation experiments was followed up using UV–visible spectrophotometer, Lambda 40, PerkinElmer, Germany.

2.8. COD Measurements. Hanna COD Meter and Multiparameter Photometer Model HI 83099 was used for the Chemical Oxygen Demand (COD) measurements. The percentages of the COD removal of MB were calculated by applying the following equation:

$$\%\ \mathrm{COD} = 100 \times \frac{(C_0 - C_t)}{C_0}, \tag{6}$$

where C_0 is the initial COD value of MB and C_t is the COD value at each time interval of sunlight irradiation.

2.9. Temperature Measurements. The temperature of the treated water was measured during the degradation experiments using Scichem Tech infrared thermometer, gun type professional, SCT658, USA. The maximum temperature achieved inside the reactor during the experiments is 50°C.

3. Results and Discussion

3.1. Preparation and Characterization of TiO_2/PET Sheets. Coating of PET with TiO_2 was conducted by dip coating method followed by exposing to mild heat and pressure. Wet PET polymeric sheets were first immersed in concentrated

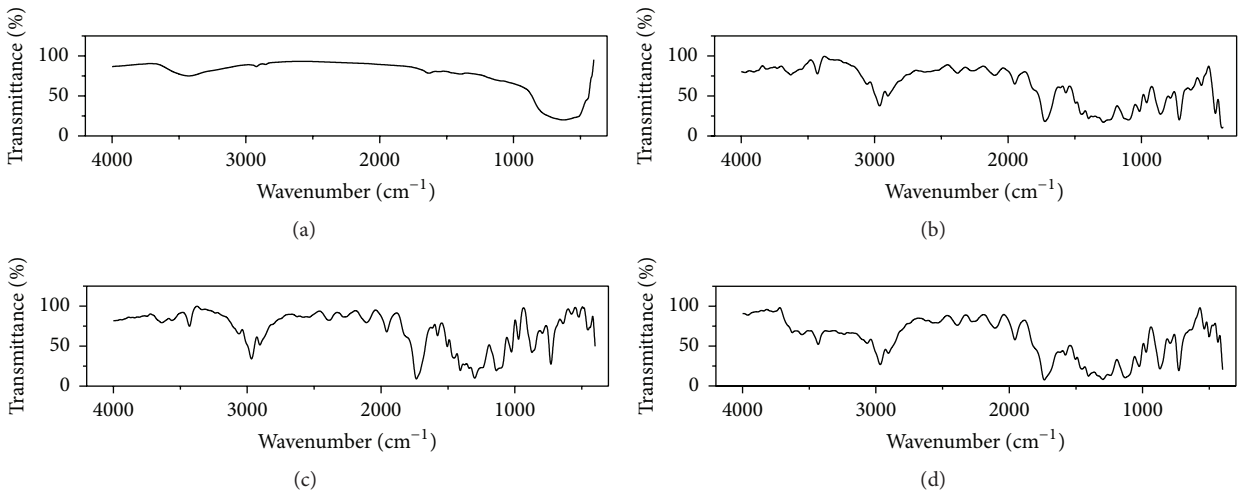

Figure 3: FT-IR spectra of (a) TiO_2, (b) pristine PET, (c) TiO_2 coated PET, and (d) solar irradiated TiO_2 coated PET.

TiO_2 solution. The TiO_2/PET sheets were then heated at 60°C under mild pressure. The mild temperature and pressure result in the dehydration of water molecules formed by the -OH groups at both PET and TiO_2 surfaces leading to successful binding between the adsorbed TiO_2 and PET substrate.

After coating PET sheet with TiO_2 for the first time, the TiO_2 content was found to be 30.5%. Washing with water reduced the TiO_2 content to 26.4% and 25% for one and two times, respectively. From the third to fifth washing, the TiO_2 content decreased slightly from 24.8% to 24.1%. Further washings result in no further leaching.

The FT-IR spectra of TiO_2 and pristine PET and TiO_2 and coated PET are given in Figures 3(a)–3(c). As shown in Figure 3(a), the primary O-H stretching of the hydroxyl functional group appeared at 3427 cm^{-1}. Besides, the band around 1630 cm^{-1} is attributed to the bending vibration H-OH groups. For pristine PET (Figure 2(b)), the main characteristic peaks are as follows: (a) strong peak at 1731 is due to carbonyl group, (b) peak at 3630 cm^{-1} is assigned to end hydroxyl group, and (c) the peak at 3431 cm^{-1} is attributed to overtone vibration of carbonyl group. After coating with TiO_2 (Figure 3(c)), the peak assigned to hydroxyl group was shifted to 3639 cm^{-1} due to bonding with PET.

In addition, SEM measurements also reveal the successful preparation of TiO_2/PET sheets. SEM images of TiO_2, pristine PET, and TiO_2 coated PET are depicted in Figures 4(a)–4(c). As shown in Figure 4(b), pristine PET appeared as smooth yarns. However, after coating (Figure 4(c)), TiO_2 nanoparticles appeared to be homogeneously distributed on PET yarns.

3.2. Solar Photocatalytic Degradation of MB. Under the sunlight irradiation, remarkable changes in the color of MB solution were noticed. Complete decolorization was achieved within 5 hours of light illumination. The change in color was followed up spectrophotometrically. Figure 5(a) shows the change in the absorption spectrum of MB solution with time of illumination. The corresponding measured solar UV doses during the whole experiment are indicated in Figure 5(b). As shown in Figure 5(a), all peaks in the absorption spectrum of MB decrease as the time of illumination increases suggesting the complete mineralization of MB molecules. It is also worthy to mention that the treated MB solutions were clear during the whole degradation experiment. No suspended TiO_2 particles were observed and consequently there is no need for the separation step. This indicates the efficient performance of the prepared TiO_2/PET sheets.

After complete decolorization, the recirculating colorless MB solution was left for 2 hours for further sunlight exposure. COD of all collected samples were then measured. The results indicated the complete mineralization of the MB molecules (Figure 6).

The complete photomineralization of MB using films of titania has been demonstrated as given in the following equation [35]:

$$C_{16}H_{18}N_3SCl + 25.5O_2 + h\nu \longrightarrow HCl + H_2SO_4 + 3HNO_3 + 16CO_2 + 6H_2O \quad (7)$$

It is clear from Figures 5 and 6 that the mineralization process occurs on a longer time than the oxidative photobleaching of MB. It has been previously also found that the measurement of the rate of photobleaching of MB is expected not to be equivalent to the rate of mineralization of the dye, which is usually a slower process [1].

3.3. Durability of the TiO_2/PET Sheets. Reuse of TiO_2/PET sheets for the photocatalytic degradation of MB inside the CPC reactor was investigated. The solar photodegradation experiments using the same TiO_2/PET sheets were repeated using fresh MB solutions. TiO_2/PET showed a high durability for 7 repetitions at 7 daylights. Comparison between the different photocatalytic experiments during the 7 days was made using the normalized illumination time ($t_{30\,w}$) as shown previously in (4). Complete decolorization of fresh MB solutions occurred at approximately $t_{30\,w}$ = 300 min at the first 5 days (Figure 7). The rates of MB photobleaching during

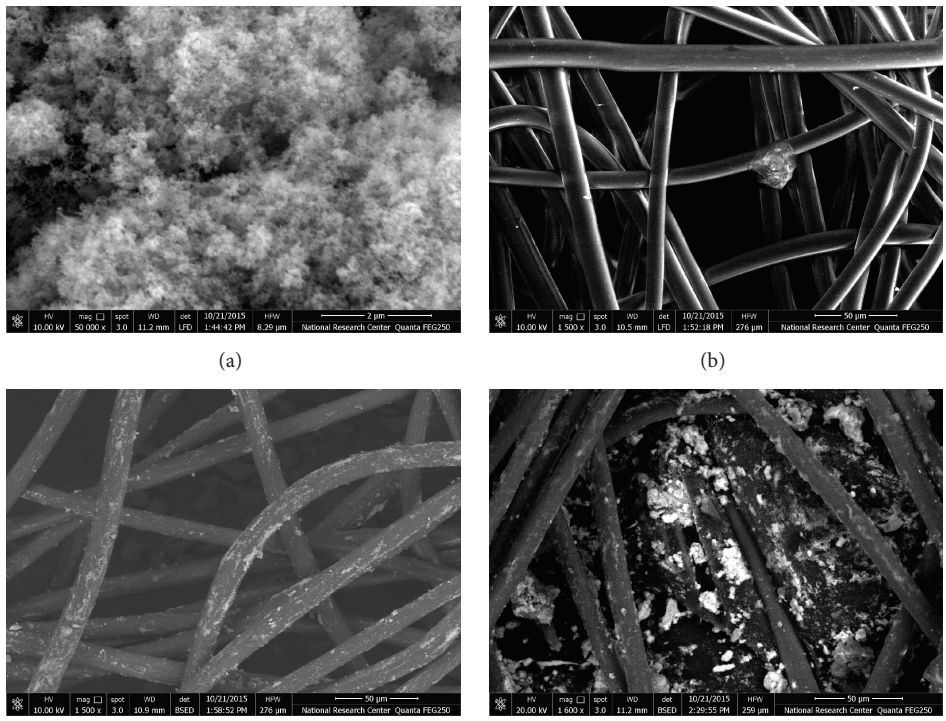

(a) (b) (c) (d)

Figure 4: SEM images of (a) TiO_2, (b) pristine PET, (c) TiO_2 coated PET, and (d) solar irradiated TiO_2 coated PET. Bars in (a) and (b)–(d) = 2 μm and 50 μm, respectively.

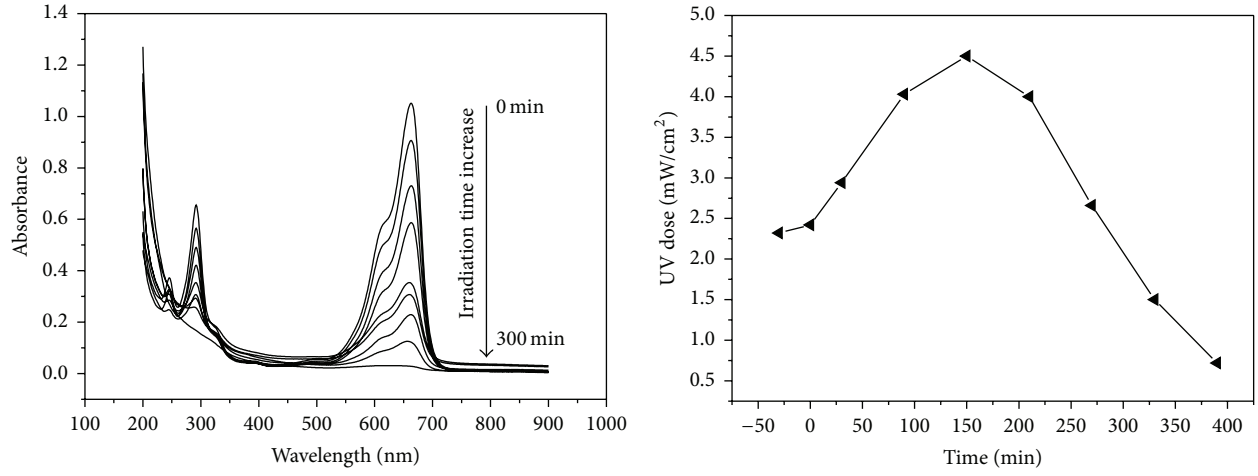

(a) (b)

Figure 5: (a) Change in the absorption spectrum of MB solution within 5 hours of illumination and (b) the measured solar UV doses at different time intervals of the degradation experiment.

the first to the fifth runs nearly coincided (not shown here). However, as shown in Figure 7, at runs 6 and 7, the rate of photobleaching became slower. No more decolorization was observed for MB solutions after 7 repetitions. On the other side, the color of TiO_2/PET sheets appeared white after first 3 repetitions. This means that, at early use of TiO_2/PET sheets, both adsorbed and dissolved MB molecules were involved in the photooxidative reactions. However, as the number of repetitions increases, the sheets' color turns toward deep blue. The initial amounts of adsorbed MB molecules on TiO_2/PET sheets at each repetition were calculated according to (5) and listed in Table 1. These experimental and visual observations suggest that the extra adsorption of MB dye on TiO_2/PET sheets results in blocking the photocatalytically active sites of TiO_2 particles.

The physicochemical characteristics of TiO_2/PET sheets were investigated before and after the solar photodegradation experiments. Figure 3(d) represents the IR spectrum of TiO_2/PET sheets after 7 repetitions. As shown in Figure 3(d), no change was observed in the main characteristic peaks of

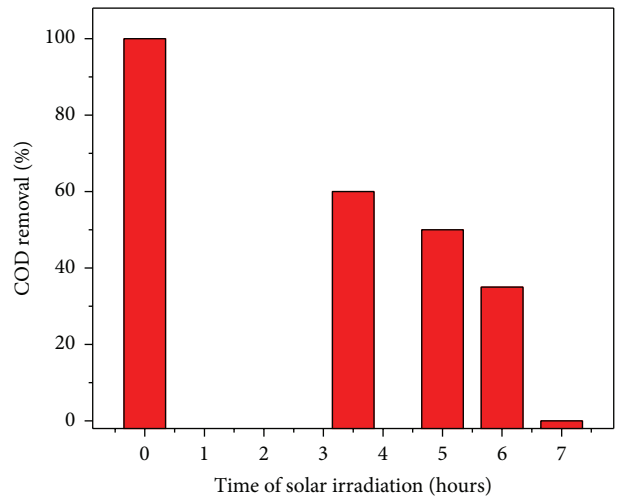

Figure 6: The change in the COD removal percentage at different intervals of irradiation time.

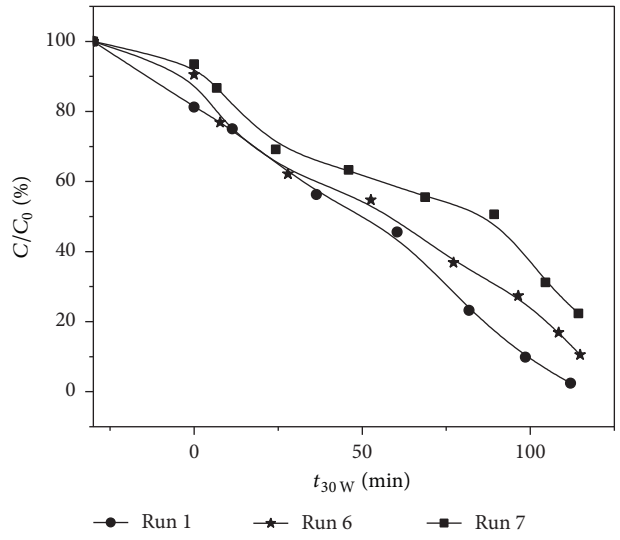

Figure 7: Decolorization of MB as a function of $t_{30\,W}$ (illumination time) on TiO_2/PET surface at different repetitions.

Table 1: The initial amount of adsorbed MB molecules on TiO_2/PET sheets at different repetitions.

Number of repetitions	Amount of adsorbed MB (mg/m^2)
1	24.4
2	24.1
3	23.9
4	18.2
5	18.5
6	12.1
7	8.3

the composite. However, the vibrational peak of carbonyl group in PET at 869 cm^{-1} is slightly shifted to 871 cm^{-1}. This shift corresponds to the surface complexation of MB and PET through functional groups (-CO) via hydrogen bonding.

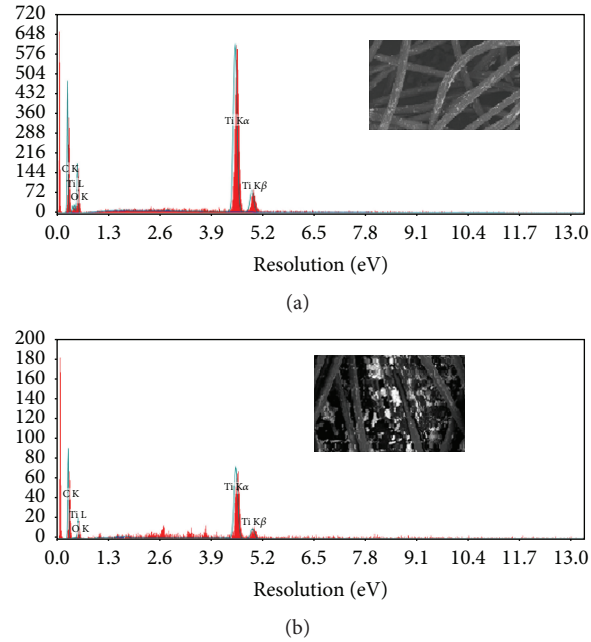

Figure 8: EDX spectra of (a) TiO_2 coated PET and (b) solar irradiated TiO_2 coated PET.

Besides, some agglomeration for TiO_2 particles was observed by SEM measurements on PET surfaces after 7 repetitions (Figure 4(d)). On the other hand, EDX spectroscopy reveals the good binding of TiO_2 to PET surfaces. As shown in Figures 8(a) and 8(b), the two characteristic signals of Ti atom at 4.6 and 5 eV were observed in the EDX spectra of TiO_2/PET sheets. EDX data indicated that the percentage amounts of TiO_2 on PET surfaces were 42.17 and 36.54%, respectively. This means that only 6% of TiO_2 was lost after seven cycles giving rise to both the high performance and durability of the prepared composite.

4. Conclusions

A home-made designed and fabricated bench-scale solar CPC recirculating photocatalytic reactor has been utilized for the photocatalytic oxidation of organic pollutants. Evonik TiO_2 Aeroxide P25 immobilized on PET was prepared via an effective cost method. The photocatalytic performance of TiO_2/PET sheets was tested using MB as a model pollutant. COD analyses reveal the complete mineralization of MB. Durability of TiO_2/PET composite was also tested under sunlight irradiation. TiO_2/PET showed good durability. Results indicate only 6% reduction in the amount of TiO_2 after seven cycles. No remarkable change was observed for the physicochemical characteristics of TiO_2/PET after the irradiation processes.

Abbreviations

A: The cross-sectional area of the annulus, m^2
a: Inner radius of used glass tube, m
b: Radius of used Teflon rode, m
C: A constant, which depends on the ratio a/b, dimensionless

C_{cpc}: The CPC concentration ratio, dimensionless
COD: Chemical oxygen demand, mg/L
D_e: Equivalent diameter, m
C_0: The initial COD value of MB, mg/L
C_{0A}: Concentration of MB in solution after the dark adsorption, mg
C_{0B}: Concentration of MB in solution before the dark adsorption, mg
C_t: The COD value at each time interval of sunlight irradiation, mg/L
EDX: Energy dispersive X-ray
f: The friction factor, dimensionless
FT-IR: Fourier transform infrared
g: The local acceleration due to gravity, m/s^2
h_f: The head loss due to friction, m
k: Kelvin temperature, degree
L: The length of the pipe, m
$\dot{m}$: The mass flow rate, kg/s
N: Number of PET strips
MB: Methylene blue
PET: Polyethylene terephthalate
R_e: Reynolds number, which is a quantity used to characterize different flow regimes (laminar or turbulent), dimensionless
t_n: The experimental time for each withdrawn sample, min
$t_{30\,w}$: Normalized illumination time at UV power of 30 W/m^2
S: Area of PET strip, m^2
SEM: Scanning electron microscope
UV: Ultraviolet
$\overline{UV}$: The average solar ultraviolet radiation, W/m^2
V: The mean velocity of the fluid, m/s
V_i: The irradiated volume of the MB solution, L
V_T: The total volume of the treated MB solution, L
W_1: Weights of PET substrate before loading with TiO_2, g
W_2: Weights of PET substrate after loading with TiO_2, g
ρ: The density of the fluid, kg/m^3
μ: The dynamic viscosity of the fluid kg/(m·s)
π: A mathematical constant, the ratio of a circle's circumference to its diameter, commonly approximated as 3.14159
δ: The distance of CPC arc, m
θ_a: The half angle of acceptance, degree
λ_{max}: Wavelength at the maximum absorption value of MB, nm.

Conflict of Interests

The authors declare that there is no conflict of interests regarding the publication of this paper.

Acknowledgments

The Science and Technology Development Fund (STDF), Egypt, Grant no. 4746, supports this work financially.

References

[1] A. Mills, C. Hill, and P. K. J. Robertson, "Overview of the current ISO tests for photocatalytic materials," *Journal of Photochemistry and Photobiology A: Chemistry*, vol. 237, pp. 7–23, 2012.

[2] Y. Dong, Z. Bai, R. Liu, and T. Zhu, "Preparation of fibrous TiO_2 photocatalyst and its optimization towards the decomposition of indoor ammonia under illumination," *Catalysis Today*, vol. 126, no. 3-4, pp. 320–327, 2007.

[3] O.-H. Park and H.-Y. Na, "Photocatalytic degradation of toluene vapour using fixed bed multichannel photoreactors equipped with TiO_2–coated fabrics," *Environmental Technology*, vol. 29, no. 9, pp. 1001–1007, 2008.

[4] D. M. EL-Mekkawi and H. R. Galal, "Removal of a synthetic dye "Direct Fast Blue B2RL" via adsorption and photocatalytic degradation using low cost rutile and Degussa P25 titanium dioxide," *Journal of Hydro-Environment Research*, vol. 7, no. 3, pp. 219–226, 2013.

[5] M. Saif, S. M. K. Aboul-Fotouh, S. A. El-Molla, M. M. Ibrahim, and L. F. M. Ismail, "Improvement of the structural, morphology, and optical properties of TiO_2 for solar treatment of industrial wastewater," *Journal of Nanoparticle Research*, vol. 14, article 1227, 2012.

[6] M. P. Paschoalino and W. F. Jardim, "Indoor air disinfection using a polyester supported TiO_2 photo-reactor," *Indoor Air*, vol. 18, no. 6, pp. 473–479, 2008.

[7] D. Mihailović, Z. Šaponjić, M. Radoičić et al., "Functionalization of polyester fabrics with alginates and TiO_2 nanoparticles," *Carbohydrate Polymers*, vol. 79, no. 3, pp. 526–532, 2010.

[8] K. Sawada, M. Sugimoto, M. Ueda, and C. H. Park, "Hydrophilic treatment of polyester surfaces using TiO_2 photocatalytic reactions," *Textile Research Journal*, vol. 73, no. 9, pp. 819–822, 2003.

[9] M. Saif, S. A. El-Molla, S. M. K. Aboul-Fotouh et al., "Synthesis of highly active thin film based on TiO_2 nanomaterial for self-cleaning application," *Spectrochimica Acta Part A: Molecular and Biomolecular Spectroscopy*, vol. 112, pp. 46–51, 2013.

[10] S. A. Khalil and A. M. Shaffie, "Prediction of clear-sky biologically effective erythematic radiation (EER) from global solar radiation (250–2800 nm) at Cairo, Egypt," *Advances in Space Research*, vol. 51, no. 9, pp. 1727–1733, 2013.

[11] J. I. Ajona and A. Vidal, "The use of CPC collectors for detoxification of contaminated water: design, construction and preliminary results," *Solar Energy*, vol. 68, no. 1, pp. 109–120, 2000.

[12] E. R. Bandala, C. A. Arancibia-Bulnes, S. L. Orozco, and C. A. Estrada, "Solar photoreactors comparison based on oxalic acid photocatalytic degradation," *Solar Energy*, vol. 77, no. 5, pp. 503–512, 2004.

[13] M. Kus, W. Gernjak, P. F. Ibáñez, S. M. Rodríguez, J. B. Gálvez, and S. Icli, "A comparative study of supported TiO_2 as photocatalyst in water decontamination at solar pilot plant scale," *Journal of Solar Energy Engineering*, vol. 128, no. 3, pp. 331–337, 2006.

[14] A. M. Amat, A. Arques, F. López, and M. A. Miranda, "Solar photo-catalysis to remove paper mill wastewater pollutants," *Solar Energy*, vol. 79, no. 4, pp. 393–401, 2005.

[15] O. Prieto, J. Fermoso, Y. Nuñez, J. L. del Valle, and R. Irusta, "Decolouration of textile dyes in wastewaters by photocatalysis with TiO_2," *Solar Energy*, vol. 79, no. 4, pp. 376–383, 2005.

[16] S. Malato, J. Blanco, D. C. Alarcón, M. I. Maldonado, P. Fernández-Ibáñez, and W. Gernjak, "Photocatalytic decontamination and disinfection of water with solar collectors," *Catalysis Today*, vol. 122, no. 1-2, pp. 137–149, 2007.

[17] S. Singh, H. Mahalingam, and P. K. Singh, "Polymer-supported titanium dioxide photocatalysts for environmental remediation: a review," *Applied Catalysis A: General*, vol. 462-463, pp. 178–195, 2013.

[18] H. S. Hafez, A. El-Hag Ali, and M. S. A. Abdel-Mottaleb, "Photocatalytic efficiency of titanium dioxide immobilized on PVP/AAc hydrogel membranes: a comparative study for safe disposal of wastewater of Remazol Red RB-133 textile dye," *International Journal of Photoenergy*, vol. 7, no. 4, pp. 181–185, 2005.

[19] A. A. Essawy, A. E.-H. Ali, and M. S. A. Abdel-Mottaleb, "Application of novel copolymer-TiO_2 membranes for some textile dyes adsorptive removal from aqueous solution and photocatalytic decolorization," *Journal of Hazardous Materials*, vol. 157, no. 2-3, pp. 547–552, 2008.

[20] Y. Ma and J.-N. Yao, "Comparison of photodegradative rate of rhodamine B assisted by two kinds of TiO_2 films," *Chemosphere*, vol. 38, no. 10, pp. 2407–2414, 1999.

[21] B. Henkel, T. Neubert, S. Zabel et al., "Photocatalytic properties of titania thin films prepared by sputtering versus evaporation and aging of induced oxygen vacancy defects," *Applied Catalysis B: Environmental*, vol. 180, pp. 362–371, 2016.

[22] Z.-A. Lin, W.-C. Lu, C.-Y. Wu, and K.-S. Chang, "Facile fabrication and tuning of TiO_2 nanoarchitectured morphology using magnetron sputtering and its applications to photocatalysis," *Ceramics International*, vol. 40, no. 10, pp. 15523–15529, 2014.

[23] Y. Yin, R. Huang, W. Zhang, M. Zhang, and C. Wang, "Superhydrophobic-superhydrophilic switchable wettability via TiO_2 photoinduction electrochemical deposition on cellulose substrate," *Chemical Engineering Journal*, vol. 289, pp. 99–105, 2016.

[24] W. Mekprasart, T. Khumtong, J. Rattanarak, W. Techitdheera, and W. Pecharapa, "Effect of nitrogen Doping on optical and photocatalytic properties of TiO_2 thin film prepared by spin coating process," *Energy Procedia*, vol. 34, pp. 746–750, 2013.

[25] S. Cabanas-Polo and A. R. Boccaccini, "Electrophoretic deposition of nanoscale TiO_2: technology and applications," *Journal of the European Ceramic Society*, vol. 36, no. 2, pp. 265–283, 2016.

[26] J. A. Byrne, B. R. Eggins, N. M. D. Brown, B. McKinney, and M. Rouse, "Immobilisation of TiO_2 powder for the treatment of polluted water," *Applied Catalysis B: Environmental*, vol. 17, no. 1-2, pp. 25–36, 1998.

[27] J. Kasanen, M. Suvanto, and T. T. Pakkanen, "UV stability of polyurethane binding agent on multilayer photocatalytic TiO_2 coating," *Polymer Testing*, vol. 30, no. 4, pp. 381–389, 2011.

[28] Y. Paz, "Application of TiO_2 photocatalysis for air treatment: patents' overview," *Applied Catalysis B: Environmental*, vol. 99, no. 3-4, pp. 448–460, 2010.

[29] A. Mills, N. Elliott, I. P. Parkin, S. A. O'Neill, and R. J. Clark, "Novel TiO_2 CVD films for semiconductor photocatalysis," *Journal of Photochemistry and Photobiology A: Chemistry*, vol. 151, no. 1–3, pp. 171–179, 2002.

[30] M. Keshmiri, M. Mohseni, and T. Troczynski, "Development of novel TiO_2 sol-gel-derived composite and its photocatalytic activities for trichloroethylene oxidation," *Applied Catalysis B: Environmental*, vol. 53, no. 4, pp. 209–219, 2004.

[31] P. Du, J. T. Carneiro, J. A. Moulijn, and G. Mul, "A novel photocatalytic monolith reactor for multiphase heterogeneous photocatalysis," *Applied Catalysis A: General*, vol. 334, no. 1-2, pp. 119–128, 2008.

[32] L. L. P. Lim, R. J. Lynch, and S.-I. In, "Comparison of simple and economical photocatalyst immobilisation procedures," *Applied Catalysis A: General*, vol. 365, no. 2, pp. 214–221, 2009.

[33] M. A. Henderson, "A surface science perspective on TiO_2 photocatalysis," *Surface Science Reports*, vol. 66, no. 6-7, pp. 185–297, 2011.

[34] I. Sopyan, M. Watanabe, S. Murasawa, K. Hashimoto, and A. Fujishima, "A film-type photocatalyst incorporating highly active TiO_2 powder and fluororesin binder: photocatalytic activity and long-term stability," *Journal of Electroanalytical Chemistry*, vol. 415, no. 1-2, pp. 183–186, 1996.

[35] R. W. Matthews, "Photocatalytic oxidation and adsorption of methylene blue on thin films of near-ultraviolet-illuminated TiO_2," *Journal of the Chemical Society, Faraday Transactions 1: Physical Chemistry in Condensed Phases*, vol. 85, no. 6, pp. 1291–1302, 1989.

[36] J. Ryu and W. Choi, "Substrate-specific photocatalytic activities of TiO_2 and multiactivity test for water treatment application," *Environmental Science & Technology*, vol. 42, no. 1, pp. 294–300, 2008.

[37] B. Tryba, M. Toyoda, A. W. Morawski, R. Nonaka, and M. Inagaki, "Photocatalytic activity and OH radical formation on TiO_2 in the relation to crystallinity," *Applied Catalysis B: Environmental*, vol. 71, no. 3-4, pp. 163–168, 2007.

[38] J. B. Galvez and S. Malato, *Solar Detoxification*, UNESCO Publishing, Paris, France, 2003.

[39] P. Ellenberger, *Piping and Pipeline Calculations Manual: Construction, Design Fabrication and Examination*, Elsevier, Philadelphia, Pa, USA, 2014.

[40] R. H. Perry and D. W. Green, *Perry's Chemical Engineers Handbook*, vol. 6, McGraw-Hill, 1984.

[41] F. M. White, *Fluid Mechanics*, McGraw-Hill, New York, NY, USA, 7th edition, 2011.

[42] S. Malato, J. Blanco, A. Vidal et al., "Applied studies in solar photocatalytic detoxification: an overview," *Solar Energy*, vol. 75, no. 4, pp. 329–336, 2003.